Korean J. Chem. Eng., 36(8), 1267-1273 (2019)
DOI: 10.1007/s11814-019-0321-z

pISSN: 0256-1115
eISSN: 1975-7220

Synergistic effect of blended primary and secondary amines functionalized onto the silica on CO_2 capture performance

Clinton Manianglung, Rose Mardie Pacia, and Young Soo Ko†

Department of Chemical Engineering, Kongju National University,
1223-24 Cheonan-daero, Seobuk-gu, Cheonan-si, Chungcheongnam-do 31080, Korea
(*Received 30 April 2019 • accepted 5 June 2019*)

Abstract−Amine-functionalized silica sorbents were synthesized by blending (3-aminopropyl)trimethoxysilane (1NS-P) and [3-(methylamino)propyl]trimethoxysilane (1NS-S) of varying proportions and incorporating it in the support via incipient wetness technique. Adsorption characteristics were examined at a design adsorption temperature of 30 °C. The blended amine adsorbents exhibited higher CO_2 adsorption capacity (5.6-6.4 wt%) and CO_2/N efficiency (0.47-0.48) than 1NS-P and 1NS-S. Among the blended amine adsorbents synthesized in this work, 1NS-PS-50, which has 50% primary amine and 50% secondary amine, is the most ideal for post-combustion CO_2 capture application because it has high CO_2 adsorption capacity, high CO_2/N efficiency, and better performance than its diamine counterpart, N-[3-(trimethoxysilyl)propyl]ethylenediamine.

Keywords: Blended Amine, Incipient Wetness, Amine-functionalized Silica, Adsorption, CO_2 Capture

INTRODUCTION

Anthropogenic CO_2 has been directly correlated with the issue of global warming; thus, efforts have been dedicated to mitigating this primary source. Post-combustion capture (PCC) is a set of end-of-pipe technologies established as a viable method to reduce CO_2 from the exhaust of combustion process [1]. Various techniques, such as cryogenic distillation, membrane separation, absorption using aqueous solutions, and adsorption using solid adsorbents, have been developed to achieve an optimum and efficient PCC process [2,3]. Though absorption by means of aqueous amine solvent is the most commonly used and is the mature technology of PCC in a large-scale application [4], it consumes a large amount of energy for regeneration, with further drawbacks such as low CO_2 loading capacity, high equipment corrosion rate, large equipment size requirement, and loss of solvent in regeneration [5]. Recently, adsorption via novel solid sorbents has received widespread attention for being capable of reversibly capturing CO_2 from flue gas streams, with advantages of reduced energy requirement for regeneration, greater capacity, higher selectivity, and ease of handling [6].

A number of materials were employed as adsorbents, such as activated carbon, carbon nanotubes, zeolites, molecular sieves, metal-organic frameworks (MOFs), alkali-metal carbonate-based solid sorbents, and amine-functionalized silica [7]. Among these, the latest emerged as promising material. Wet impregnation and chemical grafting are typical methods of immobilization of amines in silica. To overcome the arduous preparation and low amine loading via chemical grafting, another non-conventional method of functionalization has been used, incipient wetness technique or dry impregnation. This method does not need a solvent and proceeds at a lower temperature and short time. This technique utilizes water present inside the pores of silica for the substitution of alkoxy group of aminosilane to hydroxyl and additional polycondensation reactions among OH substituted aminosilanes [8].

Amines used in the synthesis of these adsorbents are commonly classified based on the number of substituents of the amine groups (primary, secondary, tertiary) and based on the number of nitrogen atoms (mono, di, tri, multi). Monoamines with different functionalities were concluded to have varied effects on the mechanism of CO_2 adsorption [10]. Primary amine is highly reactive to CO_2, thus has high reaction rate. However, it requires high energy during desorption because of the high stability of the carbamate formed during adsorption [11]. Carbamate is a CO_2-induced product of primary or secondary amines with a neighboring amine (Fig. 1(a)). CO_2 is transiently bonded to primary or secondary amines as a carbamic acid and then converts to carbamate by adjacent amine [12]. In addition, primary amines react with CO_2 at high temperature to form urea (Fig. 1(b)), causing a reduction in capacity after several adsorption-desorption cycles. Secondary amine is more basic than primary amine, thus also exhibits high reactivity to CO_2. But steric hindrance lowers its chemisorption capacity to form a carbamate, leading to a larger amount of free amine for CO_2 adsorption [13]. Its primary advantage is that it does not react with CO_2 at high temperature to form urea; hence, it is easier to handle in the regeneration stage. Tertiary amine cannot directly react with CO_2 in dry conditions to form carbamates, resulting in a pure physisorption process. It does, however, undergo acid-base neutralization when it reacts with CO_2 in the presence of water to form bicarbonate compounds (Fig. 1(c)). Compared to carbamates which are formed via 1 : 2 ratio of CO_2 and amine, bicarbonates only require 1 : 1 CO_2 to amine ratio in its formation so tertiary amine has potentially higher adsorption capacity [14]. It is less thermally

†To whom correspondence should be addressed.
E-mail: ysko@kongju.ac.kr

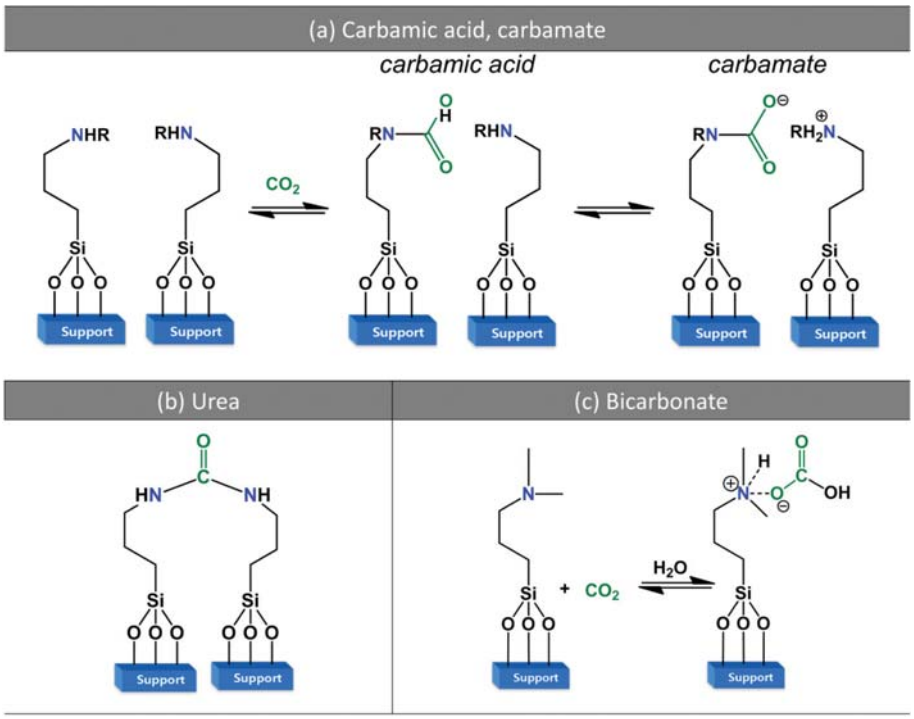

Fig. 1. Products of the reaction of CO_2 with amines of different functionalization.

stable so it would consume lesser energy in the desorption process [15]. Yet, it is not an ideal choice in PCC applications for its reaction with CO_2 is slow compared with primary and secondary amines [16].

Though these amines are of great help for CO_2 capture, the pursuit of the best amine that can satisfy all the aspects of CO_2 capture is still underway. One way of achieving this is through the blended amine system. Blending aims to maximize the individual potentials of the amines while minimizing their shortcomings [17]. The most common blended amine system consists of an amine with high Lewis basicity which has high reaction rate (primary or secondary amine) and an amine with low heat of regeneration required (tertiary or hindered amine) [18].

In our past studies [19,20], we utilized (3-aminopropyl)trimethoxysilane (primary aminosilane) and [3(methylamino)propyl]trimethoxysilane (secondary aminosilane), functionalized individually in the pores of silica. We found that the secondary aminosilane was stable in cyclic operations with no decrease in capacity. With the advantages of the abovementioned aminosilanes and the success of blending amines, in this work, amine-functionalized silica adsorbents were synthesized by blending those aminosilanes (primary and secondary, hindered) of varying ratios and incorporating them chemically in the support via incipient wetness technique. Then, CO_2 adsorption experiments were conducted to examine the adsorption characteristics of the adsorbents.

EXPERIMENTAL

1. Materials

Aqueous silica sol (YGS-30, Young Il Chemical Co., Ltd.) and fumed silica (konasil300, OCI) were used for the synthesis of the silica support. Aminosilanes used for the preparation of the amine-

Table 1. Structure of the amino organosilanes used in the preparation of the adsorbents

Amino organosilane	Structure
(3-Aminopropyl)trimethoxysilane, 1NS-P	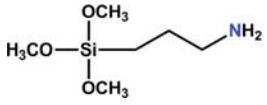
[3-(Methylamino)propyl]trimethoxysilane, 1NS-S	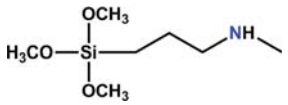
N-[3-(Trimethoxysilyl)propyl]ethylenediamine, 2NS	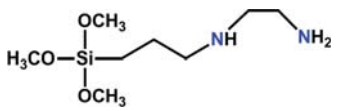

functionalized silica adsorbents were (3-aminopropyl)trimethoxysilane (1NS-P, 97% purity, Aldrich), [3(methylamino)propyl]trimethoxysilane (1NS-S, 97% purity, Aldrich), and N-[3-(trimethoxysilyl)propyl]ethylenediamine (2NS, 97% purity, Aldrich), structures are shown in Table 1. Nitrogen gas (Daesung Industrial Gases, 99.999%), carbon dioxide gas (PSG Corp., 99.999%) and air gas (MS Dong Min Specialty Gases, 99.999%) used were all ultra-high purity grade. Nitrogen gas was further purified using Fisher RIDOX column and molecular sieve 5A/13X column for the purpose of adsorbent preparation. Other reagents and gas were used without further purification.

2. Preparation of Adsorbents

The amorphous SiO_2, konasil 80, was prepared by mixing 30 wt% solid aqueous silica sol with fumed SiO_2 at 2 : 8 weight ratio. Water was then added to the mixture to make a total dispersion of 10% by weight SiO_2. The resulting dispersion was homogenized for 3 min and then spray-dried. Lastly, the dried silica was calcined for 5 hr at 500 °C [21]. The resulting konasil 80 was further treated by adding 5 mL water per gram of konasil 80, then boiling the mixture for 6 hours at 95 °C. Successively, the mixture was filtered and dried overnight at 105 °C. The resulting silica was labeled as kona80B. The textural properties of silica were analyzed using BET (Brunauer-Emmett-Teller) method and were found to have a pore volume of 1.3 cm^3/g and surface area of 265 m^2/g.

Two adsorbents were synthesized using pure primary (1NS-P) and secondary (1NS-S) aminosilanes. Three more adsorbents were synthesized using blends of the two aminosilanes and were labeled 1NS-PS-X, where X is the mmol% of primary aminosilane in the mixture. Aminosilane (6 mmol) was incorporated per gram of silica via incipient wetness technique. For the blended aminosilane, calculated amounts of the primary and secondary aminosilanes were first mixed in a separate vial. Then, the mixture was added dropwise into a flask containing kona80B, where the temperature was maintained at 50 °C and allowed to react for three hours under nitrogen atmosphere. The adsorbent was then dried overnight at 60 °C.

3. Determination of Silane Content

The nitrogen content of the sorbents was determined by Flash 2000 organic elemental analyzer. Subsequently, the %N from the elemental analysis (EA) was used to calculate the silane content using Eq. (1).

$$\text{silane content}\left(\frac{\text{mmol}}{\text{g}}\right) = \frac{\%\text{N from EA}}{100}\times\frac{1\text{ mol}}{14.01\text{ g}}\times\frac{1000\text{ mmol}}{1\text{ mol}}\times\frac{1\text{ mmol amine}}{\text{mmol N}} \quad (1)$$

4. CO_2 Single Sorption Capacity Measurement

The CO_2 sorption capacity of the adsorbents was acquired using Thermogravimetric analyzer (TGA, SDT Q600, TA Instruments). In a typical run, about 50 mg of the sample was placed in a Pt pan and was degassed at 150 °C for 1 h under flowing N_2 at 60 mL/min. The sample was then cooled to 30 °C and allowed to equilibrate for 30 min. After which, the gas flow was switched to 60 mL/min of 17% CO_2/83% N_2 gas mixture for the CO_2 sorption capacity measurement for 60 min.

5. Cyclical Performance

The cyclical adsorption/desorption stability and the effect of oxygen were investigated by temperature swing adsorption (TSA) process in the TGA. The sample was pretreated and stabilized under the same conditions as for CO_2 single sorption capacity measurement. Then the gas flow was switched to 60 mL/min of the desired gas mixture where adsorption was allowed to take place for 10 min. After which, the temperature was ramped at a rate of 10 °C/min to 150 °C, where it was left at isothermal for the desorption process to take place. Gas mixtures of 17% CO_2/83% N_2 and 17% CO_2/17% O_2/66% N_2 were used to assess the cyclical performance.

6. FT-IR Characterization

The changes in the surface characteristics of the spent adsorbents were investigated using an *in-situ* IR cell in NICOLET 6700 FT-IR Spectrometer (Thermo Scientific, USA). Prior to IR spectra measurement, the samples were formed into discs and pre-treated under vacuum for 1 h at 150 °C to eliminate pre-adsorbed H_2O and CO_2. After which, the system was then cooled to room temperature and the IR spectra were recorded with 32 scans at resolutions of 4 cm^{-1}.

RESULTS AND DISCUSSION

1. Evaluation of CO_2 Adsorption Capacity

To determine the effect of blended primary and secondary amines functionalized inside the pore of silica on CO_2 adsorption capacity, blended aminosilanes were fed to the silica during functionalization with changing molar percentage of 1NS-P to 1NS-S. The total mole of the two aminosilanes in the feed was fixed, and the molar percentages of two compounds were changed to be 100/0, 75/25, 50/50, 25/75, and 0/100, respectively.

Fig. 2 shows the single CO_2 adsorption capacity behavior of the adsorbents within 60 minutes of exposure. The CO_2 adsorption demonstrated a two-stage process. In the initial stage, capacities of the adsorbents increased linearly with time, as seen from the first four minutes. Then, the adsorption continued at a slower rate until a final uptake was apparently reached. 1NS-PS-50 showed the fast-

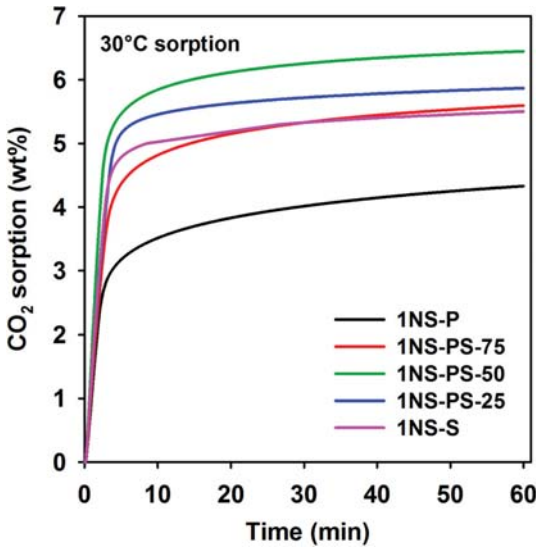

Fig. 2. CO_2 adsorption curve of the adsorbents upon exposure to 17% CO_2/83% N_2 gas mixture at 30 °C.

Table 2. CO_2 uptake loss of the adsorbents upon exposure to 17% CO_2/83% N_2 gas mixture at 30 °C for 60 min

Adsorbent	Silane content (mmol/g)[a]	CO_2 adsorption at 30 °C	
		CO_2 sorp. (wt%)[b]	CO_2/N[c]
1NS-P	3.07	4.3	0.32
1NS-PS-75	2.64	5.6	0.48
1NS-PS-50	3.07	6.4	0.47
1NS-PS-25	2.86	5.9	0.47
1NS-S	2.93	5.5	0.43

[a]Actual amine loading, calculated using Eq. (1)
[b]CO_2 sorption capacity determined by TGA with dry 17% CO_2 at 30 °C for 1 h
[c]Amine efficiency, CO_2/N ratio=amount of CO_2 adsorbed/N content

est CO_2 uptake, reaching 80% of its final uptake capacity within 3 minutes.

Table 2 summarizes the adsorption capacity and amine efficiency (CO_2/N) of the adsorbents. The functionalized silane content was calculated using Eq. (1) and the nitrogen content was assessed by elemental analysis. As seen, there was no significant change in silane content as the molar ratio of primary to secondary amines was changed, and it was in the range of 2.6-3.1 mmol/g. At an adsorption temperature of 30 °C, 1NS-S had higher sorption capacity than 1NS-P. The amine efficiency, CO_2/N ratio, showed 0.32 for 1NS-P; lower than 0.43 of 1NS-S, meaning the CO_2 capturing of 1NS-S was more efficient. CO_2 dilution had a strong effect on the amine efficiency of secondary amines but not of primary amines [22]. Compared to their ultradilute gas streams the test gas in this study was composed of 17% CO_2. This considerable increase in the CO_2 concentration could have caused the improved amine efficiency of the secondary amine, 1NS-S. Another reason could be the formation of ditethered secondary amines (Fig. 3) in the 1NS-P functionalized adsorbent. These amines, though secondary, proved to have no reactivity with CO_2 due to its rigidity, making it difficult to interact with another group by accepting a proton to form a carbamate [23]. That was why even though 1NS-P had higher silane content than 1NS-S, it had lower amine efficiency.

Very interestingly, the blended amines exhibited higher CO_2 adsorption capacity and CO_2/N efficiency than 1NS-P and 1NS-S as shown in Table 2. High CO_2 adsorption and amine efficiency of 0.47 mmol-CO_2/mmol-N were attained by 1NS-PS-50 at 30 °C. Primary and secondary amine functionalized sorbents have a maximum amine efficiency of 0.5 mmol-CO_2/mmol-N (in dry condition) because the reaction CO_2 with amine is catalyzed by another amine molecule to form unstable carbamic acid that leads to formation of carbamates (see Fig. 1(a)) [19]. Amine efficiency of 1NS-P and 1NS-S was 0.32 and 0.43, respectively, lower than the theoretical value, 0.5. Aside from the previously mentioned reasons, the higher amine efficiency of secondary amine could originate from its higher basicity. Secondary amines possess higher Lewis basicity because of an enhanced electron density, induced by the additional alkyl group near the N atom [24]. Since secondary amines react with CO_2 via acid and base reaction, this property is advantageous in capturing more CO_2. However, this advantage also led to 1NS-S not achieving the theoretical amine efficiency of 0.5. As shown in Fig. 1(a), the carbamate is formed from the reaction between amine and CO_2. The secondary amine has the freedom to rotate its methyl chain around the N atom which would occupy volumes of space and thus could hinder the access of CO_2 to the N atom [25], as compared to the primary amine. Therefore, if primary and secondary amines would be located closely next to each other (as with blended amines), the higher basicity of secondary amine could capture CO_2 easier, and the formation of carbamate with primary amine could also happen more easily due to the lesser hindrance of primary amine than secondary amine. This means under the conditions in this study, mixing the aminosilanes brought about their individual advantages in terms of CO_2 capturing. As a result, the amine efficiency of blended aminosilanes (0.47-0.48) could reach the theoretical amine efficiency, 0.5, which points to the improvement in amine efficiency with blending.

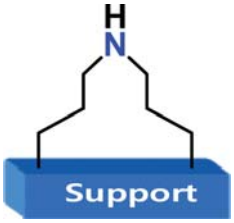

Fig. 3. Structure of ditethered secondary amine formed in the adsorbent.

2. Stability of Blended Amines

Aside from high adsorption capacity and fast adsorption kinetics, a good regenerability in adsorption/desorption operation must also be possessed by adsorbents. Furthermore, the stability of the adsorbents in the existence of flue gas impurities such as oxygen needs to be evaluated. Here, the stability was assessed in the presence of oxygen as a representative of the oxidants that could be present in flue gases. Coadsorption of CO_2 and O_2 (17% CO_2/17%

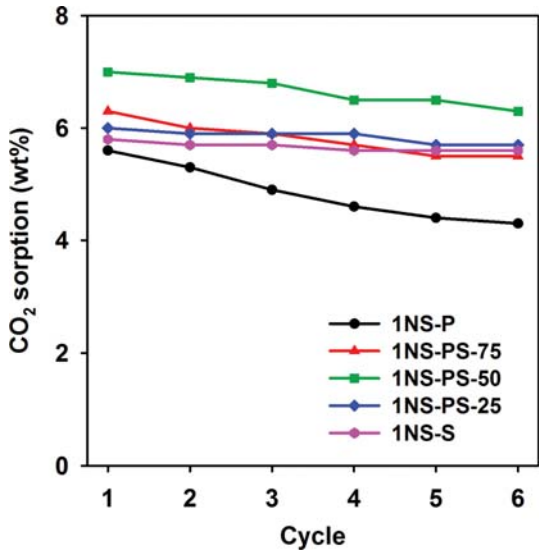

Fig. 4. CO_2 adsorption capacity of the adsorbents for TSA cycles in 17% CO_2/17% O_2/66% N_2.

Table 3. CO_2 uptake loss of the adsorbents after 6 TSA cycles in 17% CO_2/17% O_2/66% N_2

Adsorbent	Loss in CO_2 uptake (%)
1NS-P	23.2
1NS-PS-75	12.7
1NS-PS-50	10.0
1NS-PS-25	5.0
1NS-S	3.4

O_2/66% N_2) was employed over six adsorption/desorption cycles. Fig. 4 and Table 3 summarize the cyclic adsorption/desorption performance of the adsorbents. 1NS-S showed better performance (3.4% decrease in CO_2 uptake) than 1NS-P, which, in turn, experienced 23.2% decrease in its capacity. Consequently, the addition of 1NS-S to 1NS-P resulted in a more stable adsorbent. The loss in CO_2 uptake was lessened as the amount of 1NS-S was increased. Interestingly, the CO_2 uptake loss decreased drastically for 1NS-PS-75 compared to 1NS-P, suggesting that the presence of the secondary amine next to the primary amine not only improved the CO_2 adsorption capacity but also the stability of the adsorbents.

The CO_2 adsorption capacity of the adsorbents changed due to the formation of degradation species [20]. To elucidate these species, the IR spectra of the spent adsorbents (after six cycles) were measured and are illustrated in Fig. 5. It has been reported that primary amine is mainly degraded to form urea by CO_2 at a higher temperature during CO_2 ad/desorption cycles, and secondary amine is mainly degraded to form amide by oxygen at higher temperature [26]. In the O_2-induced degradation in our former work [20], it was concluded that the appearance of a peak at 1,670 cm^{-1} was due to the formation of nitrite species for primary amines and amides for secondary amines. The loss in the CO_2 uptake of 1NS-S can, therefore, be related to the presence of amides, demonstrated by the peak at 1,670 cm^{-1}. For primary amines, the main degradation product was found to be urea, evident in the high intensities of the peaks at 1,660 and 1,560 cm^{-1}. Undesorbed CO_2 in the form of carbamate from 1NS-P was also observed at 1,380, 1,510, and 1,545 cm^{-1}. These carbamates reflect the strongly adsorbed CO_2, which is a result of closely packed amine sites [27]. Aside from these CO_2-induced degradation species, just like in 1NS-S, 1NS-P had also developed a peak at 1,670 cm^{-1}, an indication of O_2-induced deactivation product in the form of nitrites.

In the case of the blended amines, it is apparent that they took after the characteristics of both the pure primary and secondary amines, as evidenced in the IR spectra (Fig. 5). A peak related to the degradation of both amines by O_2 was observed at 1,670 cm^{-1}, but with higher intensity compared to that of 1NS-S due to their combined presence in the system. While, the peaks associated with linear urea by 1NS-P were also observable at 1,660 and 1,560 cm^{-1}, but with low-intensity carbamate peaks (1,380, 1,510, 1,545 cm^{-1}). It was thus confirmed that the rise of the % decrease in CO_2 adsorption capacity as the % of primary amine increased is due to urea formation, a characteristic of primary amine degradation.

3. Comparison of the Performance of 1NS-PS-50 with 2NS

The performance of 2NS and 1NS-PS-50 was compared to investigate the effect of the presence of primary and secondary amines in the same chain differ from its mixed amine counterpart. This was one reason why this study utilized a blend of primary and secondary aminosilanes. The adsorbents underwent six ad/desorption cycles in two different gas conditions: 17% CO_2/83% N_2 and 17% CO_2/17% O_2/66% N_2. Fig. 6 displays the comparison of the cyclic performance of 2NS and 1NS-PS-50. The substantial difference between the CO_2 adsorption capacity of 2NS upon exposure to CO_2/Air mixture (33.8% loss) and CO_2/N_2 mixture (12.7% loss) suggests that the deactivation was greatly affected by O_2. In the case of 17% CO_2 in N_2, 1NS-PS-50 exhibited a marginally lower loss in CO_2 uptake than 2NS as shown in Table 4. However, CO_2

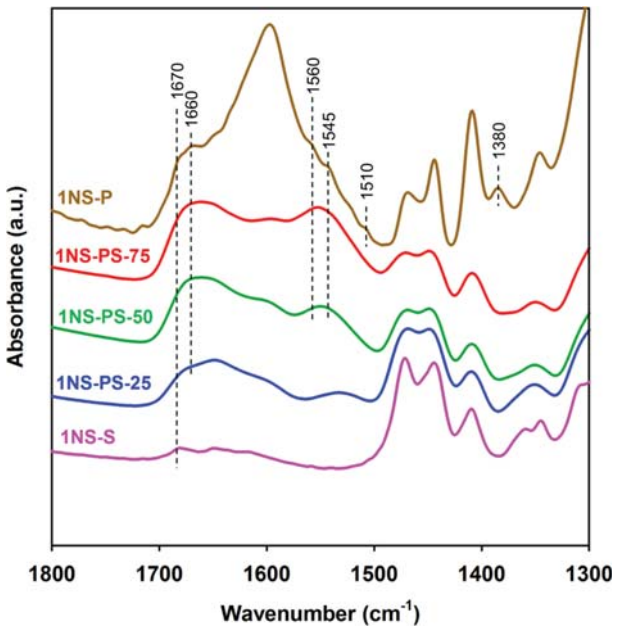

Fig. 5. FT-IR spectra of the adsorbents after 6 TSA cycles in 17% CO_2/17% O_2/66% N_2.

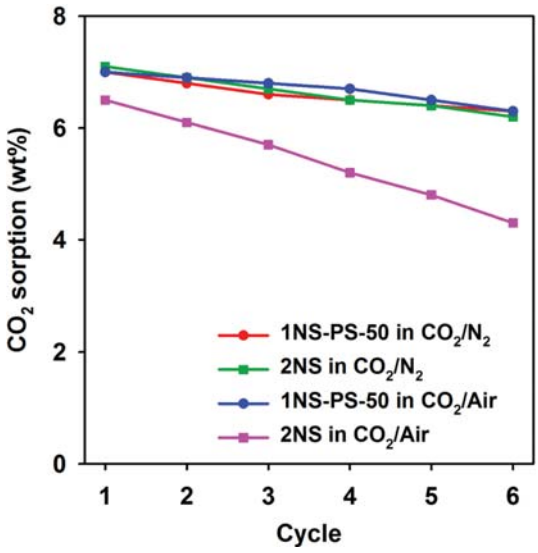

Fig. 6. CO_2 adsorption capacity of 1NS-PS-50 and 2NS in 17% CO_2/83% N_2 and 17% CO_2/17% O_2/66% N_2 gas mixtures.

Table 4. CO_2 uptake loss of 2NS and 1NS-PS-50 after 6 TSA cycles in 17% CO_2/83% N_2 and 17% CO_2/17% O_2/66% N_2 gas mixtures

Gas Condition	Adsorbent	Loss in CO_2 uptake (%)
17% CO_2/83% N_2	2NS	12.7
	1NS-PS-50	10.0
17% CO_2/17% O_2/66% N_2	2NS	33.8
	1NS-PS-50	10.0

uptake loss in 17% CO_2 in air of 1NS-PS-50 was much more stable than that of 2NS. In Fig. 7, the IR spectra of the fresh and spent adsorbents reveal the appearance of peaks at several wavenumbers which correspond to the formation of deactivation species on the adsorbents. Exposure to 17% CO_2/83% N_2 resulted in the formation of carbamates on 1NS-PS-50, reflected by the peaks at 1,545 cm^{-1}. It also developed peaks at 1,660 and 1,560 cm^{-1}, associated with linear urea because of its primary amines. Likewise, 2NS developed a high-intensity peak at 1,692 and 1,492 cm^{-1} related to cyclic urea, a degradation product of CO_2 and diamines [28]. Exposure to 17% CO_2 in air brought about the same degradation products as in those exposed to 17% CO_2 in N_2 because CO_2 was also present in the test gas employed, with the addition of amide as evidenced from the appearance of peaks at 1,670 cm^{-1}. Though primary amines are also present in 2NS, it was found in our previous study [20] that amides contribute more to the degradation of 2NS than nitrites. The higher intensity of the peaks of 2NS in this process condition support the results shown in Table 4 that its deactivation was greatly affected by O_2. Note that even a peak at 1,670 cm^{-1} appearing in 1NS-PS-50 upon exposure to CO_2/air, the peak at 1,660 cm^{-1} demonstrated a slightly lower intensity compared to CO_2/N_2 exposure. This could mean that even though an O_2-induced degradation product was formed, formation of linear urea was lessened, thereby maintaining the same loss in CO_2 uptake.

From these results, it could be inferred that covalently-bonded amines, like 2NS, are more prone to deactivation to form cyclic urea than two amines separated physically and held by van der Waals forces. Thus, 1NS-PS-50 is a better adsorbent than 2NS in terms of adsorption capacity and stability.

CONCLUSION

Konasil 80 has been modified with blended amines consisting of primary and secondary amines of varying percentages for capturing CO_2. 1NS-PS-50 had a maximized acquisition of the ideal properties of primary and secondary amines. It possesses qualities of a desirable adsorbent for application in the post-combustion CO_2 capture, such as high adsorption capacity, fast CO_2 uptake, and good stability even with the presence of oxygen. It also exhibited better performance than its diamine counterpart (2NS). In brief, the 50% primary amine/50% secondary amine blend modified silica can be used to remove CO_2 from flue gas.

ACKNOWLEDGEMENTS

This work was supported by a National Research Foundation of Korea (NRF) grant funded by the Korean government (MSIP) (2016R1D1A1B01009941). This work was also supported by the Human Resources Program in Energy Technology of the Korea Institute of Energy Technology Evaluation and Planning (KETEP), granted financial resource from the Ministry of Trade, Industry & Energy, Republic of Korea (No. 20194010201730).

REFERENCES

1. B. P. Spigarelli and S. K. Kawatra, *J. CO_2. Util.*, **1**, 69 (2013).
2. D. Aaron and C. Tsouris, *Sep. Sci. Technol.*, **40**, 321 (2005).
3. A. Olajire, *Energy*, **35**, 2610 (2010).
4. R. Huaman and S. Lourenco, *J. Fundam. Renew. Energy Appl.*, **5**, 1 (2015).
5. I. Sreedhar, T. Nahar, A. Venugopal and B. Srinivas, *Renew. Sustain. Energy Rev.*, **76**, 1080 (2017).
6. E. Sanz-Pérez, M. Olivares-Marin, A. Arencibia, R. Sanz, G. Calleja and M. Maroto-Valer, *Int. J. Greenh. Gas Control*, **17**, 366 (2013).

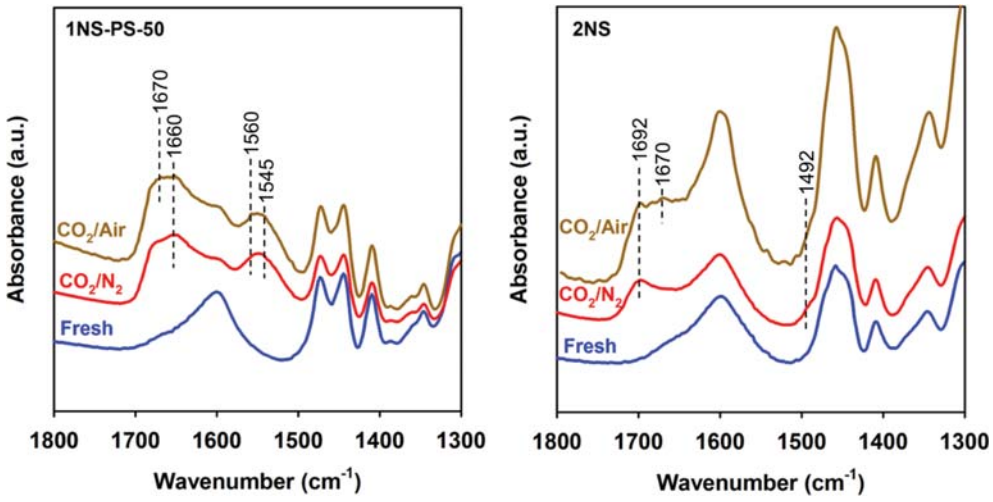

Fig. 7. FT-IR spectra of 1NS-PS-50 and 2NS before and after 6 TSA cycles in 17% CO_2/83% N_2 and 17% CO_2/17% O_2/66% N_2.

7. D. P. Bezerra, R. S. Oliveira, R. S. Vieira, C. L. Cavalcante and D. C. S. Azevedo, *Adsorption*, **17**, 235 (2011).
8. C. Chen, S. Zhang, K. H. Row and W. S. Ahn, *J. Energy Chem.*, **26**, 868 (2017).
9. B. Zhao, F. Liu, Z. Cui, C. Liu, H. Yue, S. Tang, Y. Liu, H. Lu and B. Liang, *Appl. Energy*, **185**, 362 (2017).
10. S. Ahmed, A. Ramli and S. Yusup, *Int. J. Greenh. Gas Control*, **51**, 230 (2016).
11. P. Brúder and H. F. Svendsen, *Energy Procedia*, **23**, 45 (2012).
12. C. H. Chen, D. Shimon, J. J. Lee, S. A. Didas, A. K. Mehta, C. Sievers, C. W. Jones and S. E. Hayes, *Environ. Sci. Technol.*, **51**, 6553 (2017).
13. S. Gangarapu, A. T. M. Marcelis and H. Zuilhof, *ChemPhysChem.*, **14**, 3936 (2013).
14. D. Madden and T. Curtin, *Micropor. Mesopor. Mater.*, **228**, 310 (2016).
15. W. Srisang, F. Pouryousefi, P. A. Osei, B. Decardi-Nelson, A. Akachuku, P. Tontiwachwuthikul and R. Idem, *Int. J. Greenh. Gas Control*, **69**, 52 (2018).
16. Q. Yang, M. Bown, A. Ali, D. Winkler, G. Puxty and M. Attalla, *Energy Procedia*, **1**, 955 (2009).
17. C. Nwaoha, T. Supap, R. Idem, C. Saiwan, P. Tontiwachwuthikul, M. AL-Marri and A. Benamor, *Petroleum*, **3**, 10 (2017).
18. C. Perinu, I. M. Bernhardsen, H. F. Svendsen and K. J. Jens, *Energy Procedia*, **114**, 1949 (2017).
19. J. M. Celedonio, J. H. Park and Y. S. Ko, *Res. Chem. Intermed.*, **42**, 141 (2015).
20. J. M. Celedonio, R. M. Pacia and Y. S. Ko, *Catal. Today*, **303**, 55 (2017).
21. J. H. Park, J. M. Celedonio, H. W. Seo, Y. K. Park and Y. S. Ko, *Catal. Today*, **265**, 68 (2016).
22. E. S. Sanz-Pérez, C. R. Murdock, S. A. Didas and C. W. Jones, *Chem. Rev.*, **116**, 11840 (2017).
23. D. Shimon, C. H. Chen, J. J. Lee, S. A. Didas, C. Sievers, C. W. Jones and S. E. Hayes, *Environ. Sci. Technol.*, **52**, 1488 (2018).
24. D. H. Ripin and D. A. Evans, PKa's of CH Bonds at Heteroatom Substituted Carbon & References (2014).
25. D. Fernandes, W. Conway, R. Burns, G. Lawrance, M. Maeder and G. Puxty, *J. Chem. Thermodyn.*, **54**, 183 (2012).
26. A. Heydari-Gorji and A. Sayari, *Ind. Eng. Chem. Res.*, **51**, 6887 (2012).
27. C. S. Srikanth and S. S. C. Chuang, *J. Phys. Chem. C.*, **117**, 9196 (2013).
28. W. S. Choi, K. M. Min, C. H. Kim, Y. S. Ko, J. W. Jeon, H. W. Seo, Y. K. Park and M. K. Choi, *Nat. Commun.*, **7**, 12640 (2016).